Journal Pre-proofs

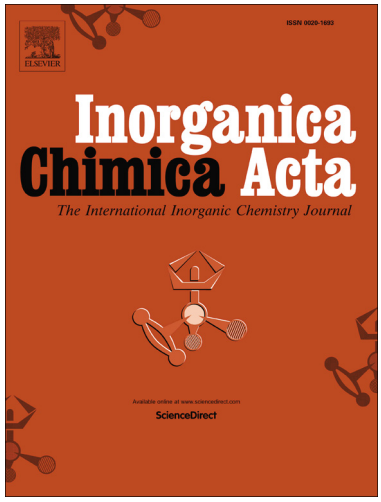

Research paper

Synthesis of a novel bipyrimidine dicarboxylic acid ligand for the preparation of panchromatic ruthenium dyes

Maria Rosana E. da Silva, Thomas Auvray, Garry S. Hanan

PII: S0020-1693(19)30680-2
DOI: https://doi.org/10.1016/j.ica.2019.119194
Reference: ICA 119194

To appear in: *Inorganica Chimica Acta*

Received Date: 13 May 2019
Revised Date: 29 August 2019
Accepted Date: 4 October 2019

Please cite this article as: M.R.E. da Silva, T. Auvray, G.S. Hanan, Synthesis of a novel bipyrimidine dicarboxylic acid ligand for the preparation of panchromatic ruthenium dyes, *Inorganica Chimica Acta* (2019), doi: https://doi.org/10.1016/j.ica.2019.119194

Synthesis of a novel bipyrimidine dicarboxylic acid ligand for the preparation of panchromatic ruthenium dyes

*Maria Rosana E. da Silva[1], Thomas Auvray[1], Garry S. Hanan[*1]*

[1]Département de Chimie, Université de Montréal, Montréal, Québec, H3T-1J4, Canada

Abstract

A novel ruthenium complex with a new 4,4'-bipyrimidine-6,6'-dicarboxylic acid ligand (H_2dcbpm) has been synthesized and its properties were investigated for application in dye-sensitized solar cells. The new dye shows a wide range of absorption of the solar spectrum with maximum of absorption at 665 nm corresponding to a 100 nm redshift compared to the precursor complex ([Ru(dcbpyH_2)$_2$(Cl)$_2$]) of the commercial N719 dye. The energies of HOMO-LUMO obtained by voltammetry and DFT calculations show an overall stabilization of the orbitals of the bipyrimidine complex compared to the bipyridine one. Despite having promising absorption properties, the redox potentials of this complex make it unsuitable for charge injection into the conduction band on TiO_2. Nevertheless, the newly prepared ligand provides an additional tuning path to adjust the energy levels of the complex in order to benefit from the red-shifted absorption it offers.

Keywords panchromatic dye, ruthenium, bipyrimidine

Introduction

Solar-to-electricity conversion is a promising approach in the optic of replacing fossil fuels by renewable energy. Indeed, the energy received by the planet in one hour corresponds to the annual energy demand worldwide. Among the different devices developed, Dye Sensitized Solar-Cell (DSSC) are particularly attractive. The current standard dyes in these cells are ruthenium complexes anchored on titanium dioxide nanoparticles. One of the most popular ruthenium complex applied in dye sensitized solar cells was reported by Grätzel *et al*. in 1991 with an overall conversion efficiency of 7.1-7.9 %.[1] Several structures were since described in the literature with enhanced efficiency and stability. Overall efficiency of 10% was reached in 2000 with the N719 dye (Figure 1) which is used today as a standard in most solar cell performance

analysis.[2] Besides, this complex shows good Incident Photon to Charge Carrier Efficiency (IPCE) in the visible, i.e. from 400 to 800 nm. Indeed, over the 480 to 600 nm region, it exhibits conversion efficiency above 80 %.[3] This dye is based on two 2,2'-bipyridine-4,4'-dicarboxylic acid (H_2dcbpy) and two thiocyanate ligands in a distorted octahedral geometry. The presence of carboxylic acid groups lowers the energy of π^* orbital of the ligand[4, 5] and the t_{2g} orbitals are destabilized due to the donor properties of thiocyanate ligands[6, 7] giving the dye a broad absorption range with maxima at 312, 395 and 535 nm in ethanol solution. The use of carboxylic acid functionalized bipyridine has also been shown to be beneficial in other applications such as photocatalyzed hydrogen production. Huijser, Vos *et al.* recently showed that the presence of ester groups on peripheral ligand of a ruthenium photosensitizer improves the catalytic activity by almost an order of magnitude when compared with its analog complex without the ester group.[8, 9]

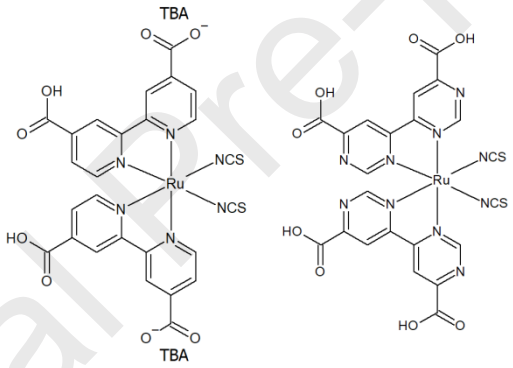

Figure 1: Chemical structure of N719 (left) and [Ru(H_2dcbpm)$_2$(SCN)$_2$] (**3b**) (right)

Over the years, efforts have been made to obtain a panchromatic dye-sensitized solar cell by employing organic dyes,[10] porphyrins,[11] co-sensitization[12] and slightly modified ruthenium complexes to absorb in the infrared region.[13] These adjustments include structural changes in the polypyridine ligand by addition of an electron withdrawing ancillary group[14] on the polypyridyl compound or introduction of donor ligands to destabilize the HOMO orbitals of the dye. In that regard, bipyrimidine can be an important class of ligands for the synthesis of new ruthenium dyes with promising ability to drive the absorption to the infrared region because of the low energy of their π* orbitals.[15] Synthesis of ruthenium complexes with 2,2' bipyrimidine and 2,2'-bipyrazine ligand have been reported in the literature.[16, 17] As shown by Ioachim *et al.* [18], homoleptic complexes based on 6,6'-disubstituted 4,4'-bipyrimidines exhibit low energy

absorption compared to $[Ru(bpy)_3]^{2+}$ due to the number of nitrogen atoms in the structure. Similarly, Ozawa *et al.* [15] described the synthesis of ruthenium sensitizers with 2,2'-bipyrimidine ligands driving the absorption of ruthenium complexes to the NIR region. These dyes show relatively large redshift of absorption maxima, which can be explained by the stabilization of the π* orbital of the ligand upon coordination to the ruthenium atom. Herein, we report a simple modification on the archetypical N3/N719 dyes based on 2,2'-bipyridine-4,4'-dicarboxylic acid by combining the incorporation of additional nitrogen in the heterocycle to extend the absorption towards the near IR region with the presence of carboxylic acid in the 6,6' positions.

Experimental Section

Materials and Methods: Solvent and chemicals were of commercial grades and used as received unless stated otherwise. Hydrated ruthenium trichloride was purchased from Pressure Chemicals. Nuclear magnetic resonance (NMR) spectra (400 MHz) were recorded in CD_3CN, D_2O/NaOD or $CDCl_3$ at room temperature (r.t.), on a Bruker AV400 spectrometer. Chemical shifts are reported in part per million (ppm) relative to residual solvent protons or carbon resonances (^1H 1.94 ppm for acetonitrile-d_3, 4.75 ppm for D_2O/NaOD and 7.27 ppm for $CDCl_3$ / ^{13}C 77.16 ppm for $CDCl_3$, 39.52 ppm for DMSO-d6). Absorption spectra were measured in acetonitrile or acetone at room temperature on a Cary 6000 UV-Vis-NIR spectrophotometer. ESI-MS data were collected on Bruker Daltonics MicrOTof. Electrochemical measurements were carried out in dry nitrogen-purged acetonitrile at room temperature with a BAS CV50W potentiostat. The working electrode was a glassy carbon electrode, the counter electrode a Pt wire and the pseudo-reference electrode a silver wire. The reference was set using an internal ferrocene sample (0.395 mV vs SCE in acetonitrile). The concentration of the analyte was about 1 mM. Tetrabutylammonium hexafluorophosphate (TBAP) was used as supporting electrolyte with a concentration of 0.10 M.

The calculations were made with Gaussian16 rev.B.01,[19] using the PBE0 hybrid functional[20] with LanL2DZ as basis set.[21-24] The optimizations were conducted without symmetry constraints, followed by frequency calculations to confirm that energy minima had been reached in all cases. GaussView6, Chemissian4.53[25] were used for data analysis, visualization and

surface plots. All calculations were performed in aqueous solution by use of the conductor like polarized continuum (CPCM) solvation model.[26]

X-Ray diffraction studies were carried out on a Bruker Venture Metaljet diffractometer using Ga-Kα radiation (λ = 1.34139 Å) and equipped with an Oxford Cryosystem liquid N_2 device set at 150 K. The cell parameters were determined from reflections taken from three sets of omega scans (104 frames, 1° per frame) using APEX3 software package.[27] Data reduction was performed with SAINT, adsorption correction with SADABS. The structure was solved via SHELXT[28] and least square refinements conducted using SHELXL[29] in Olex2.[30] The non-H atoms were refined anisotropically, using weighted full-matrix least-squares on F^2, the H-atoms were included in calculated positions and treated as riding atoms. The structure is available in the CCDC under the reference 1899174.

Synthesis: Two synthetic pathway were explored for the preparation of the ligand 6, 6'-di(furan-2-yl)- 4, 4'-bipyrimidine **2a**.

Pathway 1 for 6, 6'-di-2-furyl- 4, 4'-bipyrimidine (2a)

Synthesis of 3-(Dimethylamino)-1-(furan-2-yl)prop-2-en-1-one (1a): *N*,*N*-dimethylformamide dimethyl acetal (3.60 mL; 0.027 mol) was added dropwise into a solution of 2-furyl methyl ketone (3 g; 0.027 mol) in warm ethanol. The mixture was refluxed overnight for 12h. After that time, the solvent was removed under reduced pressure and the brown solid was crystalized in hexane giving yellow crystals whose NMR spectrum matches the literature (yield 60%).[31]

^{1}H NMR (400 MHz, $CDCl_3$) δ ppm: 7.79 (d, J=12.5 Hz, 1 H); 7.48 (s, 1H); 7.06 (d, J=3.4 Hz, 1 H); 6.47 (dd, J=3.4, 1.7 Hz, 1 H); 5.67 (d, J=12.5 Hz, 1H); 3.13 (s, 3 H); 2.92 (s, 3 H).

Synthesis of 4- (furan-2-yl) pyrimidine (1b): Product **1a** (8.63 g; 0.05 mol) and formamidine acetate (15.61 g; 0.15 mol) were refluxed in ethanol (100 mL) for 10 min. Then, sodium ethoxide (10.21 g; 0.15 mol) was added and the mixture was refluxed for 21h. After 21h, the solvent was removed under reduced pressure and the brown solid was purified on an alumina column with hexane:ethyl acetate 5:1 as eluent. The third fraction was collected, the solvent removed under reduced pressure and the resulting material was crystallized in hexane. 39% yield. The NMR spectrum matched the literature.[32]

^{1}H NMR (400 MHz, $CDCl_3$) δ ppm: 9.15 (s, 1 H); 8.72 (d, J=5.3 Hz, 1 H); 7.60 (d, J=5.3 Hz, 2 H); 7.30 (d, J=3.4 Hz, 1 H); 6.59 (m, 1 H).

Synthesis of 6, 6'-di(furan-2-yl)-4, 4'-bipyrimidine (2a): In dry THF (5 mL) 200 mg (0.0014 mol) of **1b** (5 mL) and Na (0.09 g; 0.0039 mol) were stirred at room temperature for 16h. The reaction was quenched with 5 mL of ethanol and 0.3 mL of triethylamine before being oxidized by bubbling air through the solution for 1 h. The reaction mixture was diluted in CH_2Cl_2 and washed three times with water. The organic phase was dried over $MgSO_4$ and the solvent removed under reduced pressure. Purification on a column of silica with $CHCl_3$:MeOH was performed. The solvent was removed under reduced pressure and sublimation of the solid was performed to remove traces of the starting material. Yield 6%.

^{1}H NMR (400 MHz, $CDCl_3$) δ ppm: 9.30 (d, J=1.2 Hz, 2 H); 8.73 (d, J=1.2 Hz, 2 H); 7.69 (s, 2 H); 7.40 (d, J=3.4 Hz, 2 H); 6.65 (dd, J=3.4, 1,8 Hz, 2 H).
^{13}C NMR (101 MHz, $CDCl_3$) δ ppm: 159.40; 157.36; 151.99; 146.12; 113.68; 113.18; 111.94.

Pathway 2 for 6, 6'-di(furan-2-yl)-4, 4'-bipyrimidine (2a)

Synthesis of 4-chloro-6- (furan-2-yl) pyrimidine (1c): THF (30 mL) was degassed by bubbling N_2 for 20 min. Then 565 mg (3.8 mmol), of 4,6-dichloropyrimidine, 380 mg (3.4 mmol) of furan-2-ylboronic acid and 5%mol of tetrakis(triphenylphosphine) palladium were mixed and degassed for 10 min. 720 mg (6.7 mmol) of Na_2CO_3 solubilized in 3 mL of water were then added. The solution was stirred at 70°C for 20h under N_2. The solvent was removed under reduced pressure and the desired compound was obtained after an alumina column with 5:1 hexane: ethyl acetate. Yield 52%. The NMR spectrum matched the literature[33].

^{1}H NMR (400 MHz, $CDCl_3$) δ ppm: 8.91 (s, 1 H); 7.65 (m, 2 H); 7.34 (d, J=3.4, 1 H); 6.62 (dd, J=3.4, 1.8 Hz, 1 H).

Synthesis of 6, 6'-di(furan-2-yl)-4, 4'-bipyrimidine (2a): In a round-bottomed flask, 20 mL of DMF were degassed with N_2 for 1h and then 544 mg (2.1 mmol) of triphenylphosphine, 98.6 mg (0.415 mmol) of $NiCl_2.6H_2O$ and 54 mg (0.83 mol) of zinc powder were mixed together. When the solution became brown-red, the starting material **1c** was added and the solution was stirred for 19h at 60°C. To isolate de product, DMF was removed under reduced pressure and the residue was poured in a solution of NH_4OH (30 mL, 2M) and extracted with $CHCl_3$. The solvent

was removed under reduced pressure (about 95% was removed). The resulting yellow-green oil was added dropwise in diethyl ether. The desired product precipitated and was centrifuged then washed with diethyl ether. 61% yield.

^{1}H NMR (400 MHz, $CDCl_3$) δ ppm: 9.30 (d, J=1.2 Hz, 2 H); 8.73 (d, J=1.2 Hz, 2 H); 7.69 (s, 2 H); 7.40 (d, J=3.4 Hz, 2 H); 6.65 (dd, J=3.4, 1,8 Hz, 2 H).
^{13}C NMR (101 MHz, $CDCl_3$) δ ppm: 159.40; 157.36; 151.99; 146.12; 113.68; 113.18; 111.94.
ESI-MS: Calculated 291.096 for $[M+H]^+$, Observed 291.088.

Synthesis of [4,4'-bipyrimidine]-6,6'-dicarboxylic acid (2b): In 60 mL of water (pH 10), 0.296 g (1 mmol) of **2a** was added and the mixture was set to reflux. Then 966 mg (6 mmol) of $KMnO_4$ were added and the purple mixture was refluxed for 5h. After that time the brown mixture was cooled and filtrated to remove MnO_2. Then HCl was added to the resulting solution until complete precipitation of the product as a white solid used directly in the next step. Yield 61%

^{1}H NMR (400 MHz, D_2O/NaOD) δ ppm: 9.19 (d, J=1.2 Hz, 2 H); 8.15 (d, J=1.2 Hz, 2 H).
^{13}C NMR (101 MHz, DMSO-d^6) δ ppm: 165.70; 162.59; 160.27; 158.63; 117.67
ESI-MS: Calculated 247.046 for $[M+H]^+$, Observed 247.044.

Synthesis of dimethyl[4,4'-bipyrimidine]-6,6'-dicarboxylate (2c): To obtain compound **2c**, 89 mg (0.36 mmol) of **2b** were refluxed in 20 mL of methanol with 0.2 mL of H_2SO_4 for 16h. After that, the pH of the solution was adjusted to 7 with Na_2CO_3 and the solvent was removed under reduced pressure. Water was added and the product extracted with $CHCl_3$. The solvent was removed under reduced pressure to give 56 mg of the white product. Yield 46%.
^{1}H NMR (400 MHz, $CDCl_3$) δ ppm: 9.56 (s, 2 H); 9.12 (s, 2 H); 4.10 (s, 6 H).
^{13}C NMR (101 MHz, $CDCl_3$) δ ppm: 164.52; 162.96; 159.81; 157.15; 118.19; 54.04
ESI-MS: Calculated 275.078 for $[M+H]^+$, Observed 275.180.

Synthesis of [Ru(dimethyl[4,4'-bipyrimidine]-6,6'-dicarboxylate)$_2$Cl$_2$] (3a) – Pathway 1: To obtain complex **3a**, 6 mg (0.167 mmol) of **2c**, 22 mg (0.0835 mmol) of $RuCl_3.3H_2O$ and 3,5 mg (0.0843 mmol) of LiCl were mixed in 20 mL of DMF and heated at 100°C for 22h under N_2.

DMF was removed under reduced pressure and the product was purified on column of silica with acetonitrile as eluent. Yield 10%

^{1}H NMR (400 MHz, Acetonitrile-d^3) δ ppm: 10.71 (s, 2 H); 9.24 (s, 2 H); 9.05 (s, 2 H); 8.58 (s, 2 H); 4.10 (s, 6 H); 3.94 (s, 6 H).

ESI-MS: Calculated 720.9897 for $[M+H]^+$, Observed 720.9952 ; Calculated 685.0131 for $[M-Cl]^+$, Observed 685.0136

Elemental analysis: Calculated for $C_{24}H_{26}N_8O_{11}RuCl_2$ C (%) 37.22, N (%) 14.47, H (%) 3.38, Found C (%) 37.60, N (%) 14.10, H (%) 3.45.

Synthesis of [Ru([4,4'-bipyrimidine]-6,6'-dicarboxylic acid)$_2$(SCN)$_2$] (3b): To obtain **3b,** 6 mg (8.33 μmol) of the complex **3a** and 74 mg (0.25 mmol) of KSCN were refluxed for 12h in a mix of methanol/water 6:2. After that time, 3 mL of triethylamine was added, and the reflux was maintained for an additional 5h. The solvents were then removed under reduced pressure and 2 mL of water was added. The product was precipitated with HNO_3 0.5M and the solid was centrifuged then dried under vacuum. 86 % purity by NMR.

^{1}H NMR (400 MHz, D_2O/NaOD) δ ppm: 10.05 (s, 2 H); 9.03 (s, 2 H); 8.87 (s, 2 H); 8.48 (s, 2 H).

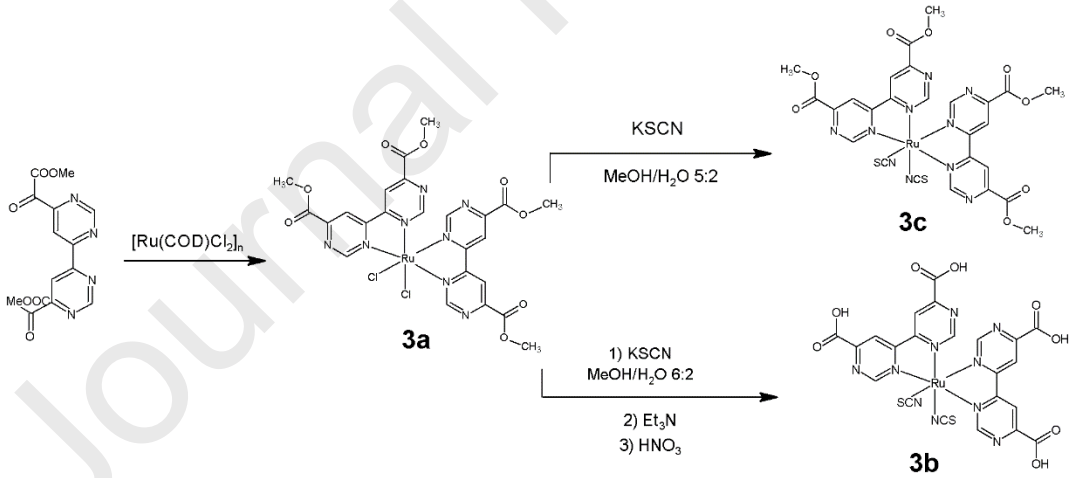

Scheme 1 Reaction pathways for the substitution of Cl^- in complex **3a** by SCN^-

Synthesis of [Ru(COD)Cl$_2$]$_n$: Following a literature procedure, 2g of $RuCl_3$,$3H_2O$ and 1.88 mL of cycloocta-1,5-diene were refluxed in 50 mL of ethanol for 24h. The resulting brown solid was filtrated and washed with ethanol and dried under vacuum. Yield 79%

Synthesis of [Ru(dimethyl[4,4'-bipyrimidine]-6,6'-dicarboxylate)$_2$Cl$_2$] (3a) – alternative synthesis : In 25 mL of DMF, 50 mg (0.182 mmol) of **2c** and 25.5 mg (0.091 mmol) of [Ru(COD)Cl$_2$]$_n$ were combined and heated under nitrogen for 24h at 100°C. Purification of the crude on silica using acetonitrile as eluent afforded **3a** with a 67% yield (33 mg).

Synthesis of [Ru(dimethyl[4,4'-bipyrimidine]-6,6'-dicarboxylate)$_2$(SCN)$_2$] (3c):
Complex **3a** (30 mg) was dissolved in a mix methanol: water 5:2 (30 mL) and to it were added 30eq. of KSCN (120 mg). The solution was then refluxed for 24h. Methanol was removed under reduced pressure until precipitation of the desired product. The dark-green solid was isolated by centrifugation, dissolved in acetonitrile (2 mL) and reprecipitated in diethyl ether, affording 26 mg of **3c**. 64% purity by NMR.
^{1}H NMR (400 MHz, Acetonitrile-d^3) δ ppm: 10.19 (s, 2 H); 9.29 (s, 2 H); 9.10 (s, 2 H); 8.61 (s, 2 H); 4.12 (s, 6 H); 3.96 (s, 6 H)
ESI-MS: Calculated 708.0194 for [M-SCN]$^+$, Observed 708.0197 ; Calculated 788.9843 for [M+Na]$^+$, Observed 788.9832.

Results and Discussion

Synthesis: The synthetic pathway chosen to prepare the targeted diester ligand **2c** involves furan functionalized ligands. Indeed, carboxylated polypyridyl ligands can be obtained via the oxidation of furanyl group using $KMnO_4$ in basic media[34]. This synthetic procedure in general has a lower ecological impact as it uses 2-furyl-methylketone which can be obtained from biomass compared to the alkyl to acid Cr^{VI} based oxidation procedure. To obtain 6,6'-di(furan-2-yl)-4,4'-bipyrimidine **2a**, two synthetic procedures were developed as illustrated in Scheme 1. The first pathway involves a known carbon-carbon coupling reaction between 4-substituted pyrimidine using sodium. First, 4-(furan-2-yl) pyrimidine **1b** was synthesized in two steps from 2-furyl-methyl ketone using *N*,*N*-dimethylformamide dimethyl acetal then formamidine acetate salt following a previously established method.[18]

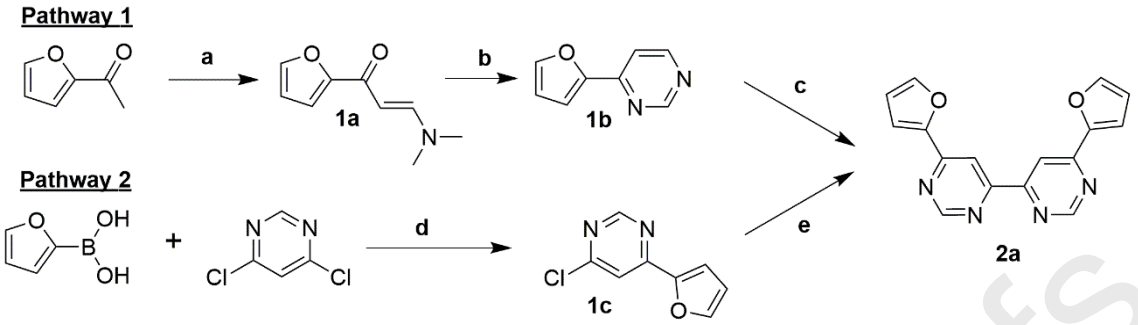

Scheme 2 Synthetic pathways towards pre-ligand **2a**

a N,N-dimethylformamide dimethyl acetal, EtOH, reflux, 12h ; **b** formamidine acetate salt, NaOEt, EtOH, reflux, 21h; **c** Na, THF, r.t., 16h ; **d** $Pd(PPh_3)_4$, Na_2CO_3, THF/H_2O, reflux, 20h ; **e** $NiCl_2{,}6H_2O$, PPh_3, Zn, DMF, 60°C, 16h

This three-step synthesis relies on economically accessible starting materials, but the final yield of the desired compound **2a** is only 6%. The low yield can be explained by undesirable side reactions involving the furanyl group, similar to reported coupling reaction[35]. One of the by-products was isolated and identified as the coupling product in which the C-C bond formation now involves the furan, leading to 4-(furan-2-yl)-6-(5-(pyrimidin-4-yl)furan-2-yl)pyrimidine (see ESI). A substantial amount of an unidentified polymer was also obtained.

Based on these complications, we thus explored another synthetic procedure in order to increase the yield of the desired product. Following the procedure described in the literature,[33] 4-chloro-6-(2-furanyl)-pyrimidine (**1c**) was obtained from a Suzuki coupling reaction and then the homocoupling was performed catalyzed by nickel[36-38] to obtain **2a** with 61% yield. From there, oxidation of the furyl groups followed by esterification of the resulting dicarboxylic acid **2b** by adapting the procedures described in the literature[39] led to ligand **2c**. The ester was prepared to avoid undesirable products during the complexation with ruthenium.

However, complexation reactions with ruthenium trichloride and the esterified ligand following procedures described in the literature[2] resulted in low yield, the by-product being mainly the homoleptic complex and a polymeric mixture similar to what was described by Rau *et al.* [40] on the synthesis of $[Ru(dtbpy)_2Cl_2]$ (dtbpy is 4,4'-di-tert-butyl-2,2'-bipyridine) (Scheme 3). We believe that the severe reaction conditions, i.e. high temperature in DMF, may lead to hydrolysis of the ester groups and consequently cause the formation of polymers through coordination of the carboxylate groups.[41]

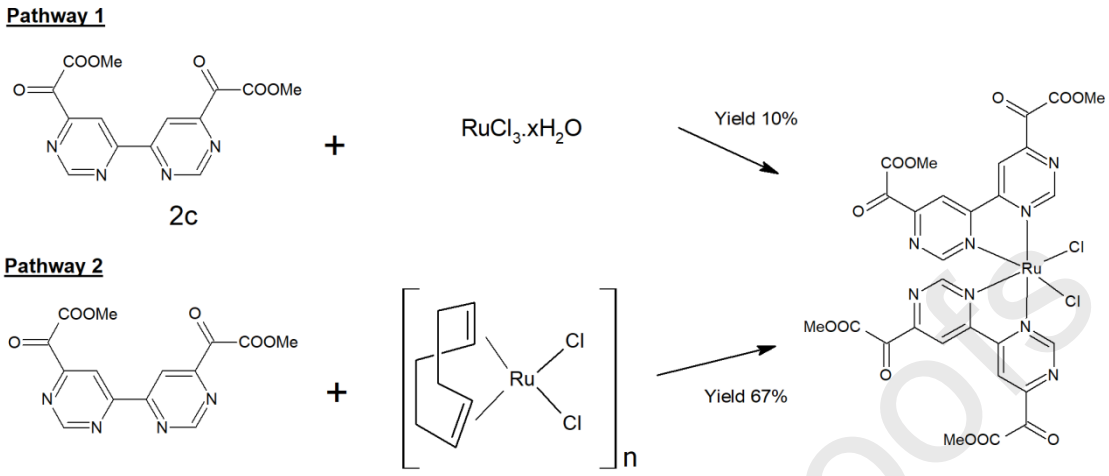

Scheme 3 Synthetic pathways towards complex **3a**

We thus explored the use of $[Ru(COD)Cl_2]_n$ (COD is cyclooctadi-1,5-ene) as starting material and obtained a better yield (67%) while working in milder conditions, i.e. at a temperature of 100°C in DMF for 24h.[42] Replacement of Cl^- by SCN^- was performed in a methanol:water 5:2 mix with 30 eq. of KSCN under reflux for 24h, but resulted in impure species.

NMR studies: ^1H NMR of complex **3a** obtained in acetronitrile-d^6 shows 4 peaks in the aromatic region from the two pyrimidine rings and two peaks at 4.10 and 3.94 ppm corresponding to the protons of the methyl groups. After substitution of Cl^- by SCN^-, all the peaks are slightly deshielded except peak A which shifts upfield to 10.19 ppm due the proximity with the more electron withdrawing SCN ligand (Figure 2). The NMR spectra of complex **3c** is however showing some impurities peaks (calculated purity of 64%). Comparison with the spectra of complex **3a** shows that there is no residual di-chloro complex. Attempts to purify **3c** by chromatography on silica, alumina or size exclusion (Sephadex-LH20) by using different solvents were not successful. Despite this, analysis of the NMR profile of the complex after replacement of chloride ligands allows to observe a shift of the signal, especially the proton A between the two nitrogen of the heterocycle pointing towards the exchanged ligands (Figure 2). By mass spectrometry, we observed the di-thiocyanate complex as the main species. We thus believe that the byproducts observed by NMR are related to the formation of isomers originated from N- or S-bounded thiocyanate[43, 44] as it is an ambidentate ligand, or anion replacement by water molecules present in the deuterated solvent.

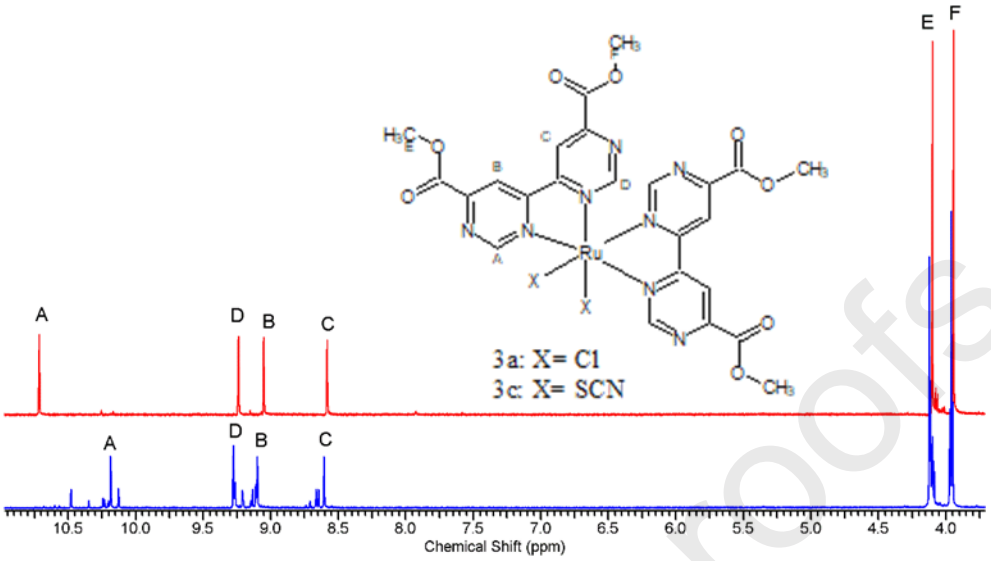

*Figure 2 [1]H NMR spectra of complexes **3a** (red) and **3c** (blue) in acetronitrile-d[3] at 400 MHz*

Crystallographic studies: We obtained green crystals suitable for single-crystal X-ray diffraction analysis for complex **3a**. The structure is shown in Figure 3. Additional data regarding the refinement parameter can be found in Table S1 and the structure is available in the CCDC under the reference number 1899174. The only structure available for the diester bipyridine equivalent does not contain atomic coordinates due to poor diffraction quality despite being obtained in a synchrotron facility[42]. We thus compared the coordination sphere within **3a** and the structure of the complex $[Ru(H_2dcbpy)_2Cl_2]$[45], see Table 1.

3a

3c

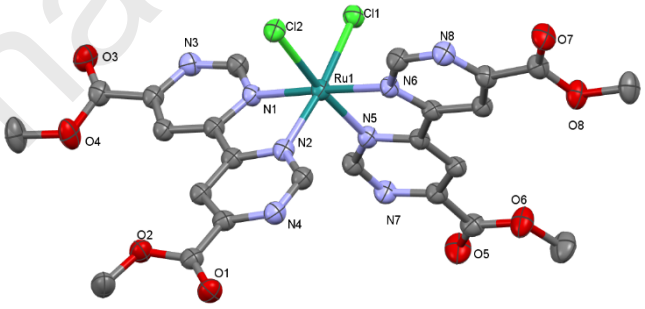

Figure 3 Ellipsoid representation of complex **3a** (50% probability, H atoms and solvents omitted for clarity)

Table 1 Selected bond lenghts and angles for **3a** and $[Ru(H_2dcbpy)_2Cl_2]$

Complex	Ru-N (Å)	Ru-Cl (Å)	N-Ru-N (°)	N-Ru-Cl (°)	Cl-Ru-Cl(°)
3a	2.039(2) 2.029(2) 2.017(2)	2.400(1) 2.385(1)	78.7(1) 100.1(2) 95.5(2) 178.0(2) 99.7(2) 78.8(2)	173.0(1) 87.5(1) 94.5(1) 87.4(1) 86.8(1) 94.2(1)	90.6(1)

	2.037(2)			87.2(1) 172.8(1)	
[Ru(H$_2$dcbpy)$_2$Cl$_2$]	2.006(3) 2.043(3) 2.029(3) 2.042(3)	2.412(1) 2.430(1)	95.4(1) 95.6(1) 79.2(1) 79.4(1) 97.8(1) 173.9(1)	173.2(1) 90.0(1) 89.3(1) 96.0(1) 88.4(1) 174.0(1) 96.0(1) 87.4(1)	86.4(1)

Comparison of the relevant bond lengths and angles allows to conclude that in both cases, the coordination environment of the Ru center is not strictly octahedral due to the restricted bite angle of the diimine ligands. This N-Ru-N bite angle is slightly tighter for the bipyrimidine ligands. Overall, the coordination sphere of the ruthenium is not affected by the modification on the diimine ligand.

UV-Vis analysis: In order to investigate the effect of the ligand modification, we measured the absorption spectra of the newly prepared complex as a first probe into their electronic properties. The values are reported in Table 2. In acetonitrile, complex **3a** exhibits three transitions. The first transition at 303 nm is attributed to a $\pi \rightarrow \pi^*$ transition and the two broad bands at 422 and 665 nm are assigned to metal-to-ligand charge-transfer (MLCT). The lower MLCT transition is redshifted by 100 nm compared to the bipyridine dicarboxylic complex [Ru(H$_2$dcbpy)$_2$(Cl)$_2$] or diester complex [Ru(Me$_2$dcbpy)$_2$(Cl)$_2$]. Looking at the corresponding thiocyanate complex, [Ru(H$_2$dcbpy)$_2$(SCN)$_2$], one can observe a slight blueshift of the absorption of about 30 nm.

Table 2 Absorption data for the complex **3a** measured in acetonitrile and relevant references

Complex	Absorption λ(max) (nm) complex (ε/10^4 M^{-1} cm^{-1})		
3a	303(2.5)	422 (1.1)	665 (1.0)
[Ru(H$_2$dcbpy)$_2$(Cl)$_2$][a]	316 (3.5)	414(1.0)	565(1.1)
[Ru(Me$_2$dcbpy)$_2$(Cl)$_2$][b]			555
[Ru(H$_2$dcbpy)$_2$(SCN)$_2$][a]	314 (4.8)	398(1.4)	538(1.4)
(TBA)[Ru(H$_3$tcterpy)(NCS)$_3$][c]	330, 344sh	429, 556sh	625
(TBA)$_3$[Ru(Htcterpy)(NCS)$_3$][d]			611 (0.7)

[a] measured in ethanol, from [2] [b] in methanol, from [42] [c] in ethanol [d] in acetonitrile, from [7] TBA tetrabutylammonium

Interestingly, if we suppose a similar shift for our complex after replacement of the chloro by thiocyanate ligand, our complex would absorb around 630 nm, corresponding to a strong redshift

compared to the absorption of the reference dye N3 [$Ru(H_2dcbpy)_2(SCN)_2$] (Table 2) and close to that of Blackdye/N749 $(TBA)_4[Ru(tcterpy)(NCS)_3]$ (H_3tctpy is [2,2':6',2''-terpyridine]-4,4',4''-tricarboxylic acid). To confirm this hypothesis, we measured the absorption spectra of the impure sample of **3c** (Figure 4-right), confirming the expected blueshift. The acid form of the complex, 3b, presents an additional blueshift (Figure S1) though the lack of purity of **3b** and **3c** prevents any further discussion.

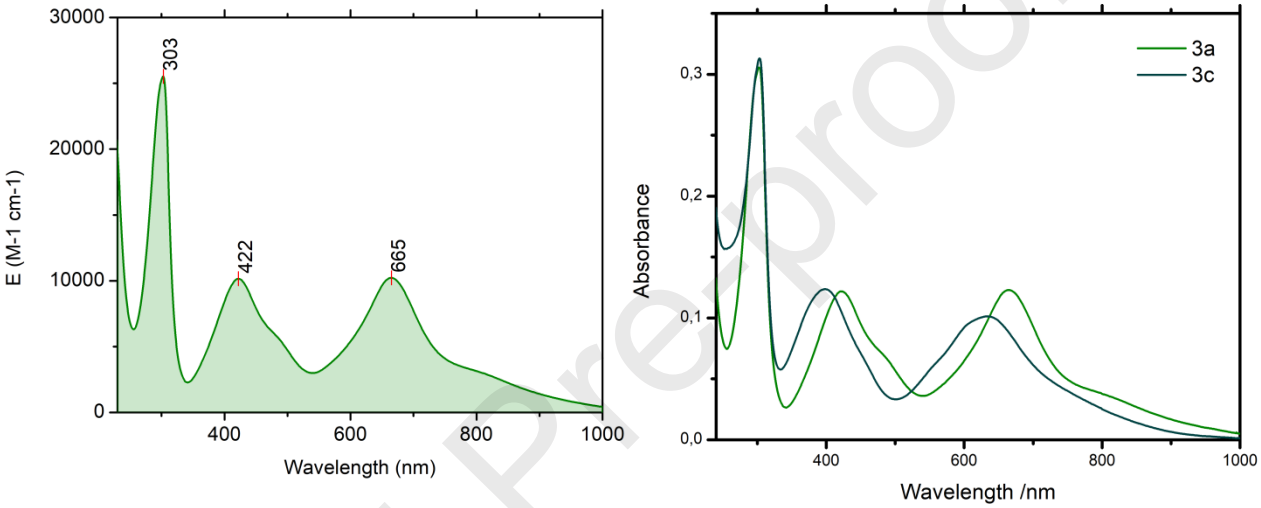

Figure 4: Absorption spectra of complexes **3a** acetonitrile (left) and comparison of the absorption spectra 3a and 3c (right)

Electrochemical studies: Complex **3a** was investigated by cyclic voltammetry, the voltammogram is presented in Figure 5. It shows a reversible oxidation wave at 0.90 V which was assigned to a metal center oxidation, i.e. the redox couple Ru(III)/Ru(II). On the cathodic side, the complex shows four reversible or quasi-reversible reduction waves corresponding to the successive reduction of the ligands at -0.53, -0.76, -1.14 and -1.27 V. These values clearly show that the bipyrimidine based complexes are much easier to reduce than the corresponding bipyridine.

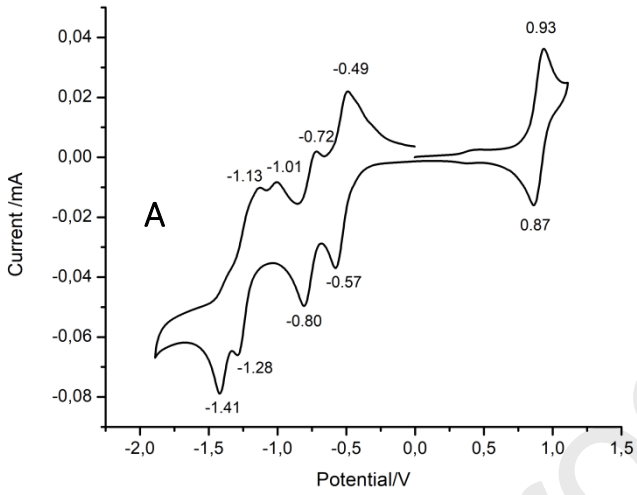

Figure 5: Voltammogram of **3a** in MeCN, $TBAPF_6$ 0,1 M (V vs SCE)

Table 3 Redox potentials obtained by cyclic voltammetry in acetonitrile (Potential in V *vs* SCE)

Complex	$E_{Ru(III)/Ru(II)}$	$E_{L/Lred}$	E_{HOMO} (eV)[c]	E_{LUMO} (eV)[c]	E_g (eV)
3a	0.90	-0.53/-0.76/-1.14/-1.27	-6.10	-4.67	1.86
$[Ru(H_2dcbpy)_2(NCS)_2]$[a]	0.85	-1.07	-6.05	-4.13	2.33
$(TBA)_4[Ru(dcbpy)_2(NCS)_2]$[b]	0.57	-1.67	-5.77	-3.53	2.43
$[Ru(H_3tcterpy)(NCS)_3]$[c]	0.67	-1.06	-5.86	-4.14	2.03

[a] from [46] [b] from [2] [c] from [7] [c] eV = - [$E_{1/2}$ - (-0.400V)] - 4.8eV (0.400V vs SCE = $E_{1/2ox}$ Fc^+/Fc).

Interestingly, analysis of complex **3c** by cyclic voltammetry offered some insight into the nature of the impurity (Figure S2). It shows an irreversible process at 0.99 V, slightly higher than for **3a** as expected. However, there is also two other quasi-reversible waves at 1.19 and 1.61 V which we attributed to the sequential Ru(III)/Ru(IV) and Ru(IV)/Ru(V) which would require a water molecule involved in these proton coupled processes[47]. The irreversibility of the first oxidation could thus be caused by related to replacement of one SCN^- by a water molecule.

Through the voltammetry data, we calculated the approximated energies of the HOMO and LUMO levels using the first oxidation and the first reduction potentials, respectively [48]. E_g was estimated from the onset wavelength of absorption spectra according to the equation $E_g = \frac{1242}{\lambda}$, where λ is the longest wavelength of absorption in nm. Based on the reduction potential, the

electron injection into the conduction band of TiO_2 would not proceed effectively because the LUMO of the bipyrimidine based dyes are lower than the conduction band of the TiO_2 (-4.05 eV) [49]. The deprotonation in the case of the H_2dcbpy complexes leads to a large shift of the reduction potential, a similar effect could bring the reduction level of our complex closer to the TiO_2 conduction band. Besides, inside the dye sensitized solar cell, these values vary as they are very sensitive to the environment. The position of the conduction band edge depends on surface charge of the semiconductor, for example. Therefore, application of the newly synthetized dye could be possible, provided modification of the surface of the semiconductor or incorporation of additives in the electrolyte to shift the Fermi level of the semiconductor[50]. It is mentioned by Boschloo *et al.* that addition of 4-*tert*-butylpyridine (TBP) to redox electrolytes used in dye-sensitized TiO_2 cells drives the TiO_2 band edge toward negative potentials[51]. On the contrary, it is reported that interfacial electron transfer are enhanced with the increase of Li^+ and H^+ concentration which could be related to the positive shift (on the electrode potential scale) of the flat band potential of TiO_2.[52, 53]

Theoretical studies: DFT calculations were performed on the fully deprotonated thiocyanate complexes - **3b** in its deprotonated form (noted **3b-H**) and N719, as reference - in water using a polarizable continuum (CPCM) and the PBE0 hybrid method combined with the LanL2DZ basis set. These complexes were chosen as they correspond to the actual species involved in the DSSC. The energy diagram is reported in Figure 6. It clearly shows the net overall stabilization in the bipyrimidine complex compared to the bipyridine one. This stabilization is more important for the LUMO (≈0.8eV) than the HOMO (≈0.3eV), following the trend observed in electrochemistry for their derivatives.

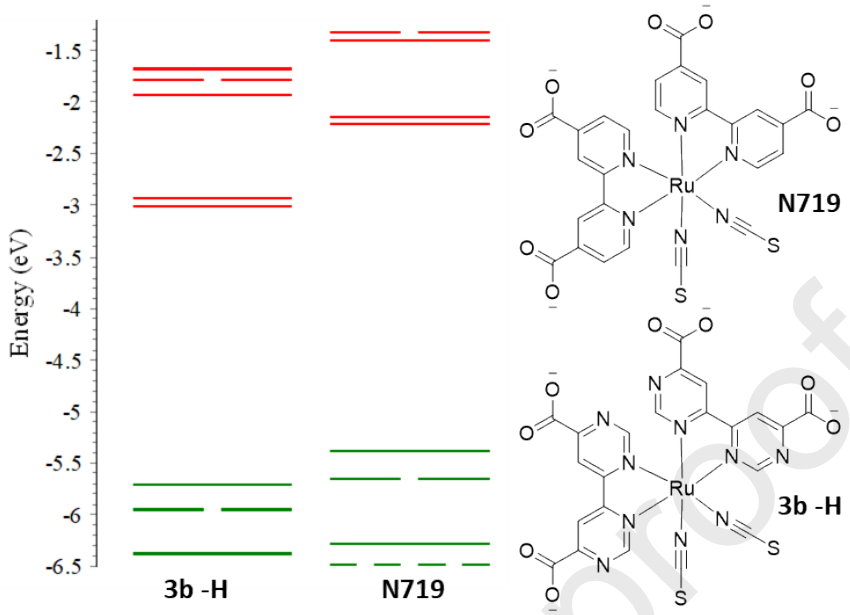

Figure 6: Energy diagram for the deprotonated form of complex **3b (3b-H)** and the reference N719 dye (green occupied orbitals, red virtual orbitals / degeneration threshold: 50meV)

Energies and contributions of each unit to the different orbitals are given in Table S2 and S3. Regarding the LUMOs, there are centered on the diimine ligands and the additional nitrogens in the cycle have the expected electron withdrawing effect which lowers them. A difference in contributions is observed in the HOMOs. The thiocyanates have an increased contribution to these orbitals, becoming the main contributing unit. In the deprotonated form of **3b**, the HOMO has a 42% Ru, 48% SCN and 10% bipyrimidine character whereas in N719, these values are 52% Ru, 36% SCN and 12% bipyridine. These variations are coherent with the bipyrimidine being a better π-accepting ligand than bipyridine, thus the lower LUMO, and indirectly leading to stabilized metal centered HOMO.

Conclusion

A new panchromatic ruthenium polypyridyl complex was synthesized and its properties were investigated related to its application in dye sensitized solar cells. Two different procedures were developed for the synthesis of the new ligand [4,4'-bipyrimidine]-6,6'-dicarboxylic acid with a significant improvement on the yield through the synthetic route that includes both a Suzuki type and a nickel catalyzed carbon-carbon coupling reaction. Likewise, a great improvement was achieved in the yield of the synthesis of complex **3a** using $[Ru(COD)Cl_2]_n$ as starting material. By

replacing the dicarboxylate-bipyridine ligands with their bipyrimidine equivalents, we obtained panchromatic Ru(II) complexes with absorption reaching into the near IR. The bipyrimidine ligands caused a substantial stabilization of the LUMOs, and of the HOMOs to a lesser extent, allowing for this red shifted absorption. Calculated energies of HOMO orbitals indicate that I^- would be able to reduce the oxidized form of the dye. However, electron injection into TiO_2 would not proceed effectively, as the LUMO energy of the dye is lower than the conduction band of the semiconductor. These results are supported by DFT calculation which shows the net overall stabilization of the deprotonated complex **3b** compared to the N719 dye. Therefore, despite having promising absorption properties, the redox potentials of this complex make it unsuitable for charge injection into the conduction band on TiO_2 and additional tuning of the energy levels is needed to benefit from the red-shifted absorption offered by the newly prepared bipyrimidine ligands.

Acknowledgments

Financial support by the Natural Sciences and Engineering Research Council of Canada is appreciated by G.S.H. M.R.E. da S. is grateful to Mitacs Globalink and Treal Technologies Inc. This research was enabled in part by support provided by Compute Canada. T.A. thanks the Faculté des Arts et Sciences at Université de Montréal for a Marguerite-Jacques-Lemay scholarship.

References

[1] B. O'Regan, M. Grätzel, Nature, 353 (1991) 737-740.
[2] M.K. Nazeeruddin, S.M. Zakeeruddin, R. Humphry-Baker, M. Jirousek, P. Liska, N. Vlachopoulos, V. Shklover, C.-H. Fischer, M. Grätzel, Inorg. Chem., 38 (1999) 6298-6305.
[3] G. Conibeer, Mater. Today, 10 (2007) 42-50.
[4] B.D. Koivisto, K.C. Robson, C.P. Berlinguette, Inorg. Chem., 48 (2009) 9644-9652.
[5] B. Pashaei, H. Shahroosvand, M. Graetzel, M.K. Nazeeruddin, Chem. Rev., 116 (2016) 9485-9564.
[6] P.A. Anderson, G.F. Strouse, J.A. Treadway, F.R. Keene, T.J. Meyer, Inorg. Chem., 33 (1994) 3863-3864.
[7] M.K. Nazeeruddin, P. Pechy, T. Renouard, S.M. Zakeeruddin, R. Humphry-Baker, P. Comte, P. Liska, L. Cevey, E. Costa, V. Shklover, L. Spiccia, G.B. Deacon, C.A. Bignozzi, M. Gratzel, J. Am. Chem. Soc., 123 (2001) 1613-1624.
[8] Q. Pan, L. Freitag, T. Kowacs, J.C. Falgenhauer, J.P. Korterik, D. Schlettwein, W.R. Browne, M.T. Pryce, S. Rau, L. Gonzalez, J.G. Vos, A. Huijser, Chem. Commun., 52 (2016) 9371-9374.

[9] T. Kowacs, L. O'Reilly, Q. Pan, A. Huijser, P. Lang, S. Rau, W.R. Browne, M.T. Pryce, J.G. Vos, Inorg. Chem., 55 (2016) 2685-2690.
[10] P. Brogdon, H. Cheema, J.H. Delcamp, ChemSusChem, 10 (2017) 3624-3631.
[11] B.L. Watson, T.A. Moore, A.L. Moore, D. Gust, Dyes Pigm., 136 (2017) 893-897.
[12] D.D. Babu, D. Elsherbiny, H. Cheema, A. El-Shafei, A.V. Adhikari, Dyes Pigm., 132 (2016) 316-328.
[13] J. Dehaudt, J. Husson, L. Guyard, F. Oswald, D. Martineau, Renewable Energy, 66 (2014) 588-595.
[14] C.C. Chou, P.H. Chen, F.C. Hu, Y. Chi, S.T. Ho, J.J. Kai, S.H. Liu, P.T. Chou, J. Mater. Chem. A, 2 (2014) 5418-5426.
[15] H. Ozawa, H. Kawaguchi, Y. Okuyama, H. Arakawa, Eur. J. Inorg. Chem., 2013 (2013) 5187-5195.
[16] D.P. Rillema, G. Allen, T.J. Meyer, D. Conrad, Inorg. Chem., 22 (1983) 1617-1622.
[17] S. Kajouj, L. Marcelis, V. Lemaur, D. Beljonne, C. Moucheron, Dalton Trans., 46 (2017) 6623-6633.
[18] E. Ioachim, E.A. Medlycott, W.G. Skene, G.S. Hanan, Polyhedron, 26 (2007) 4929-4935.
[19] M.J. Frisch, G.W. Trucks, H.B. Schlegel, G.E. Scuseria, M.A. Robb, J.R. Cheeseman, G. Scalmani, V. Barone, G.A. Petersson, H. Nakatsuji, X. Li, M. Caricato, A.V. Marenich, J. Bloino, B.G. Janesko, R. Gomperts, B. Mennucci, H.P. Hratchian, J.V. Ortiz, A.F. Izmaylov, J.L. Sonnenberg, Williams, F. Ding, F. Lipparini, F. Egidi, J. Goings, B. Peng, A. Petrone, T. Henderson, D. Ranasinghe, V.G. Zakrzewski, J. Gao, N. Rega, G. Zheng, W. Liang, M. Hada, M. Ehara, K. Toyota, R. Fukuda, J. Hasegawa, M. Ishida, T. Nakajima, Y. Honda, O. Kitao, H. Nakai, T. Vreven, K. Throssell, J.A. Montgomery Jr., J.E. Peralta, F. Ogliaro, M.J. Bearpark, J.J. Heyd, E.N. Brothers, K.N. Kudin, V.N. Staroverov, T.A. Keith, R. Kobayashi, J. Normand, K. Raghavachari, A.P. Rendell, J.C. Burant, S.S. Iyengar, J. Tomasi, M. Cossi, J.M. Millam, M. Klene, C. Adamo, R. Cammi, J.W. Ochterski, R.L. Martin, K. Morokuma, O. Farkas, J.B. Foresman, D.J. Fox, in, Gaussian 16 Rev. B.01 Wallingford, CT, 2016.
[20] C. Adamo, V. Barone, J Chem Phys, 110 (1999) 6158-6170.
[21] P.J. Hay, W.R. Wadt, The Journal of Chemical Physics, 82 (1985) 270-283.
[22] P.J. Hay, W.R. Wadt, The Journal of Chemical Physics, 82 (1985) 299-310.
[23] W.R. Wadt, P.J. Hay, The Journal of Chemical Physics, 82 (1985) 284-298.
[24] T.H.D. Jr, P.J. Hay, Mordern Theoretical Chemistry III ed., Plenum, New york, 1977.
[25] S. Leonid, V 4.53, (2005-2017) www.chemissian.com.
[26] M. Cossi, N. Rega, G. Scalmani, V. Barone, J Comput Chem, 24 (2003) 669-681.
[27] Bruker AXS Inc. APEX3, SAINT, SADABS, Madison (2016) Wisconsin USA.
[28] G.M. Sheldrick, Acta Crystallogr. Sect. A, 71 (2015) 3-8.
[29] G.M. Sheldrick, Acta Crystallogr. Sect. C, 71 (2015) 3-8.
[30] O.V. Dolomanov, L.J. Bourhis, R.J. Gildea, J.A.K. Howard, H. Puschmann, J. Appl. Crystallogr., 42 (2009) 339-341.
[31] R.J.R. Rao, A.K.S.B. Rao, K. Swapna, B.B. Rani, Y.L.N. Murthy, Asian J. Chem., 24 (2012) 1837-1843.
[32] G. Yang, Q. Jia, L. Chen, Z. Du, J. Wang, RSC Adv., 5 (2015) 76759-76763.
[33] L. Mologni, M. Dalla Via, A. Chilin, M. Palumbo, G. Marzaro, ChemMedChem, 12 (2017) 1390-1398.
[34] J. Dehaudt, J. Husson, L. Guyard, Green Chem., 13 (2011) 3337-3340.

[35] E.V. Verbitskiy, E.M. Cheprakova, E.F. Zhilina, M.I. Kodess, M.A. Ezhikova, M.G. Pervova, P.A. Slepukhin, J.O. Subbotina, A.V. Schepochkin, G.L. Rusinov, O.N. Chupakhin, V.N. Charushin, Tetrahedron, 69 (2013) 5164-5172.
[36] P.F.H. Schwab, F. Fleischer, J. Michl, J. Org. Chem., 67 (2002) 443-449.
[37] S. Dufresne, G.S. Hanan, W.G. Skene, J. Phys. Chem. B, 111 (2007) 11407-11418.
[38] G. Khalil, C. Orvain, L. Fang, L. Barloy, A. Chaumont, C. Gaiddon, M. Henry, N. Kyritsakas, P. Mobian, Dalton Trans., 45 (2016) 19072-19085.
[39] J. Husson, J. Dehaudt, L. Guyard, Nat. Protoc., 9 (2014) 21-26.
[40] S. Rau, M. Ruben, T. Büttner, C. Temme, S. Dautz, H. Görls, M. Rudolph, D. Walther, A. Brodkorb, M. Duati, C. O'Connor, J.G. Vos, J. Chem. Soc., Dalton Trans., (2000) 3649-3657.
[41] E. Eskelinen, S. Luukkanen, M. Haukka, M. Ahlgrén, T.A. Pakkanen, J. Chem. Soc., Dalton Trans., (2000) 2745-2752.
[42] M. Schwalbe, B. Schafer, H. Gorls, S. Rau, S. Tschierlei, M. Schmitt, J. Popp, G. Vaughan, W. Henry, J.G. Vos, Eur. J. Inorg. Chem., 2008 (2008) 3310-3319.
[43] T.P. Brewster, W. Ding, N.D. Schley, N. Hazari, V.S. Batista, R.H. Crabtree, Inorg. Chem., 50 (2011) 11938-11946.
[44] M.K. Nazeeruddin, M. Grätzel, J. Photochem. Photobiol., A, 145 (2001) 79-86.
[45] T. Fujihara, A. Kobayashi, M. Iwai, A. Nagasawa, Acta Crystallogr. Sect. E, 60 (2004) m1172-m1174.
[46] M.K. Nazeeruddin, A. Kay, I. Rodicio, R. Humphry-Baker, E. Mueller, P. Liska, N. Vlachopoulos, M. Graetzel, J. Am. Chem. Soc., 115 (1993) 6382-6390.
[47] J.C. Dobson, T.J. Meyer, Inorg. Chem., 27 (1988) 3283-3291.
[48] M.M. Ahmida, S.H. Eichhorn, ECS Trans., 25 (2010) 1-10.
[49] J.I. Fujisawa, T. Eda, M. Hanaya, Chem. Phys. Lett., 685 (2017) 23-26.
[50] A. Hagfeldt, G. Boschloo, L. Sun, L. Kloo, H. Pettersson, Chem. Rev., 110 (2010) 6595-6663.
[51] G. Boschloo, L. Haggman, A. Hagfeldt, J. Phys. Chem. B, 110 (2006) 13144-13150.
[52] Z.-S. Wang, T. Yamaguchi, H. Sugihara, H. Arakawa, Langmuir, 21 (2005) 4272-4276.
[53] G. Redmond, D. Fitzmaurice, J. Phys. Chem., 97 (1993) 1426-1430.

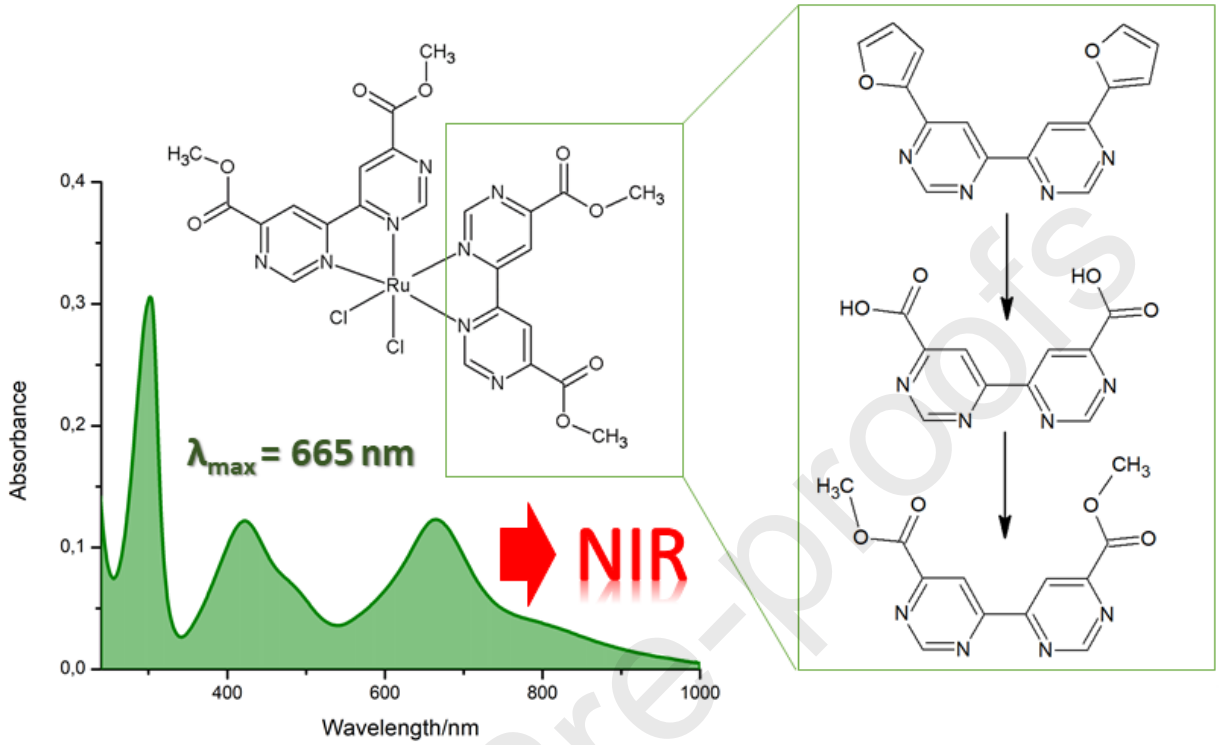

- 4,4’-Bipyrimidine-6,6’-dicarboxylic acid ligand forms Ru(II) complexes.
- Red-shifted absorption to 665 nm.
- Ambidentate isomerisation of the thiocyanate Ru(II) complex.